# A set of indices based on indentation tests for assessment of rock cutting performance and rock properties

## by H. Copur, N. Bilgin, H. Tuncdemir, and C. Balci*

### Synopsis

Experimental studies for quantification of force and brittleness indices relevant to rock cutting performance are presented. A simple interpretation method is developed, which quantifies the force-penetration response obtained from indentation tests. Basic parameters of the quantification are force increment and decrement rates, force increment and decrement periods, and number of increment and decrement data points. Blocks of eleven different rock samples were collected from different operating mines in Turkey and subjected to indentation tests to calculate the indices. The samples included harzburgite, serpentinite, trona, limestone, claystone, two different sandstone samples, siltstone and three different chromite ore samples. The concept was validated by a set of full-scale linear cutting tests using a conical cutter for measuring the cutting performance in relieved and unrelieved conditions, i.e. cutter forces, specific energy, size distribution of rock cuttings. The rock cuttings were sieved to determine coarseness index, indicates coarse chip generation characteristics, and size distribution. The force index is moderately correlated with the cutting performance and mechanical properties of the rocks, and poorly correlated with the coarseness index and size distribution of cuttings. A general and moderate trend is observed between the brittleness index and the coarseness index, cutting performance for unrelieved cutting conditions and mechanical properties of the rocks. However, additional data is required to fill the data gaps and to potentially establish relationship between the brittleness index and all other parameters.

## Introduction

Mechanical excavation is currently the only alternative to drill and blast. The increasing restrictions on the drill and blast method and the inherent advantages of mechanical excavation, such as continuous operation and possibility of automation, are the major reasons leading to an increase in the use of mechanical miners in the mining and civil construction industries. Designing faster and better excavation systems and developing accurate and reliable performance prediction models would improve the success of mechanical mining.

Cuttability of rocks means resistance to cutting by mechanical tools such as pick cutters and roller cutters. The cuttability can be measured by full-scale linear cutting tests, and some index tests requiring core samples, such as small-scale cutting tests, indentation tests, uniaxial compressive strength tests, Brazilian tensile strength tests, point load tests, etc.[1,2]. Based on these tests, the specific energy, which is energy required to excavate (or cut) a unit volume of rock, optimum cutting geometry, and forces acting on cutters are measured and/or predicted. Knowing these parameters helps selecting and designing mechanical miners and predicting their performance, which is used for feasibility and planning purposes[1-5].

A full-scale rock cutting test is one of the best tools for defining cuttability of rocks, since an actual rock sample is cut by a real-life cutter, which reduces the scaling effect. Its disadvantage is that it requires large blocks of rock samples (around 1×1×0.6 m), which are usually difficult, too expensive or impossible to obtain. Therefore, the core sample based cuttability tests are preferred in many cases, even though their predictive abilities are lower than full-scale rock cutting tests. Developing new index tests or test interpretation methods would improve the predictive abilities of core based cuttability tests.

Brittleness is one of the material properties related to breakage characteristics under different loading conditions. Therefore, the brittleness can be used as a cuttability parameter[6-12]. However, brittleness has not been investigated in detail, to date, from the mechanical excavation point of view.

A project supported by the Scientific and Technical Research Council of Turkey (TUBITAK) was initiated to develop a set of core sample based indices related to rock cutting mechanics[13]. Estimation of the indices (force and brittleness indices) was based on a new interpretation method of macro-scale

---

\* Istanbul Technical University, Mining Engineering Department, Maslak, Istanbul, Turkey.

# A set of indices based on indentation tests for assessment

indentation tests. These indices were correlated to rock cutting performance obtained from linear cutting tests and mechanical properties of the rocks. Part of the results of this project are presented and discussed in this paper.

## Background

There are different theoretical explanations for the rock breakage mechanism with different types of cutters (pick and roller cutters) or indentors. Some of these explanations are based on tensile fracturing, shearing, elasticity theory and/or on the plasticity theory[14-29]. In all of the cases, there are similar mechanisms: a crushed zone is created in the rock due to the high compressive stress concentrations generated by the tool. Tensile hoop stresses occur in the perimeter of the crushed zone. If the rock is brittle, hoop stress creates tensile cracks or fractures propagating outwards or towards the adjacent cutting lines. If the two cracks from adjacent cuts meet, the rock ridge between the cut lines is removed. In the case of ductile failure, shearing plays a major role instead of tensile fracture development. In reality, the mechanical rock breakage process includes, to varying degrees, tensile and shear types of failure modes, depending on rock properties, cutter and cutting geometry.

Some researchers used indentation tests to design drills and mechanical excavators and predict machine performance by assessing drillability and boreability of rock samples[29-32]. The Robbins Company, which was the largest tunnel boring machine and raise drill machine manufacturering company, used indentation tests as one of their principal tools for evaluating the boreability of rock samples with respect to designing tunnel boring machines and raise boring machines and prediction of penetration rates[31]. The main approach was to predict forces, which would act on an actual cutter, by curve fitting of the force-penetration data obtained from indentation tests. Based on the predicted forces and performance, the machine was designed. The Earth Mechanics Institute of the Colorado School of Mines, has also being used indentation tests to define rock boreability and cuttability for many years[5].

Different measures of brittleness in rock mechanics have been developed for different purposes. Elongation, fracture failure, formation of fines, ratio of compressive to tensile strength, and angle of internal friction are some examples of measures of rock brittleness[33-34]. A limited number of researchers tried to use these conventional measures of rock brittleness to correlate with mechanical rock breakage efficiency or rock cutting performance, but the results were not satisfactory[6-7, 33]. A common opinion of those researchers was that a brittleness concept relevant to mechanical excavation of rocks had to be developed.

A group of researchers developed a brittleness test to use as one of the predictive parameters for tunnel boring machine performance[11]. Another group of researchers investigated brittle and ductile failure modes by triaxial testing and connected this information with rock cutting[8-9]. Another group of researchers indicated that the performances of tunnel boring machines and rotary drills were related to the ratio of rock uniaxial compressive strength and Brazilian tensile strength[10, 32]. A researcher suggested a brittleness index as a multiplication of uniaxial compressive strength

and Brazilian tensile strength, and indicated a correlation between the index and percussive and rotary blast hole drilling performance[35-36]; he also stated a correlation between the coarseness index of rock cuttings and percussive drilling performance[37].

Many investigations with micro-scale indentation testing were also performed for understanding brittle characteristics of man-made materials such as ceramics and glasses[38-41]. A researcher demonstrated the relationship between the machinability (cuttability) and brittleness of glass ceramics[41]. He indicated that the specific cutting energy and chip size increased with the increase of brittleness of the glass ceramics.

## Concept of force and brittleness indices

Some researchers[30] stated that ductile rocks yielded relatively flatter (smoother) force-penetration graphs after macro-scale indentation tests, Figure 1. Similar behaviour was observed
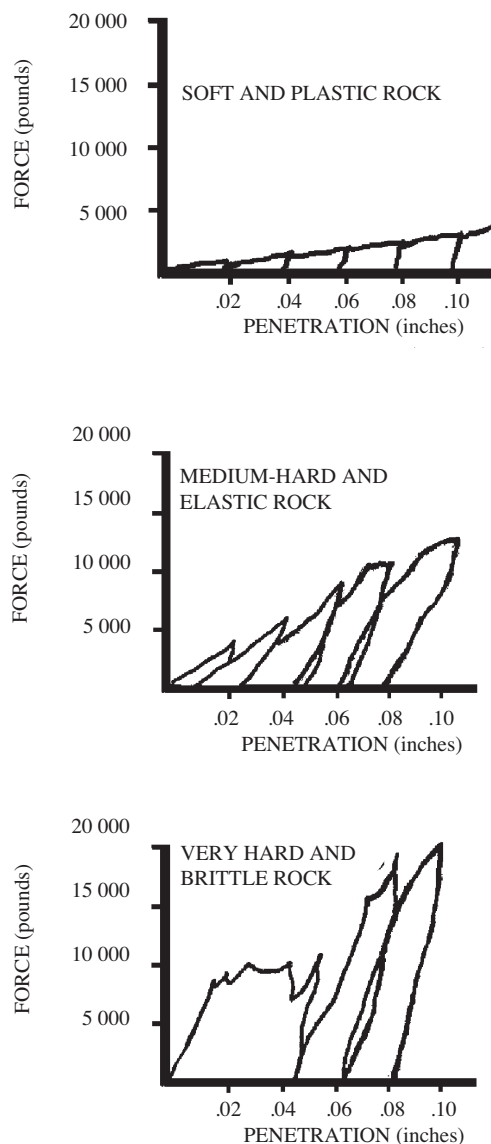


**Figure 1—Visual brittleness classification based on force-penetration graphs[30]**

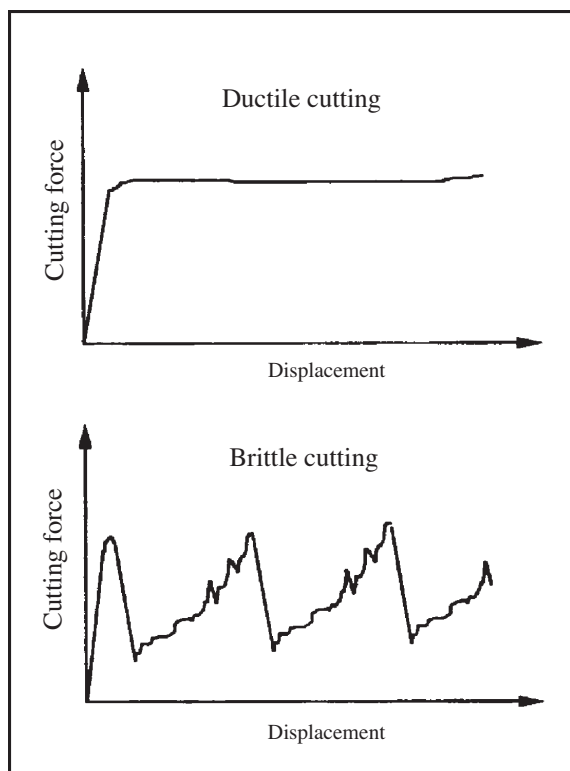# A set of indices based on indentation tests for assessment



Figure 2—Idealization of ductile and brittle rock cutting data[8]



Figure 3—Nomenclature for force increment and decrement rates and periods (hypothetically generated for this study)

in the force-penetration graphs from linear cutting tests[8], Figure 2. However, these definitions of brittleness were based on visual observations on force-penetration responses; and therefore, they could be considered as qualitative.

The authors cited above[30, 8] consider that if the rock being loaded is comparatively more brittle, it yields relatively more fluctuated force-penetration due to chipping, which means less fluctuation for more ductile rocks. Shapes of force-penetration response depend also on the micro (texture, grain geometry, matrix material) and macro (strength, elasticity) properties of rocks, geometry of indentor (sharpness, shape, dimension), and some environmental parameters (type of loading, temperature, confinement amount and material, data sampling rate). In addition to the authors cited above[30, 8], Paul and Sikarski[21] and Miller and Sikarski[22] mention the importance of force increase (increment) rates based on their experimental and theoretical studies.

It could be concluded, based on all of these studies, that the shape of force-penetration response might be considered as an indicator of rock breakage characteristics. The authors of this paper explain below their ideas about quantification of the force-penetration response.

If force-penetration graphs of indentation tests are visually observed, it is seen that force increments take some certain periods see Figure 3, which is generated hypothetically for this study. A force increment period is followed by a force drop (or force decrement period) due to chipping. If a material is more prone to breakage or shows brittle characteristics, it might break frequently and violently after taking mostly elastic and some plastic deformation.
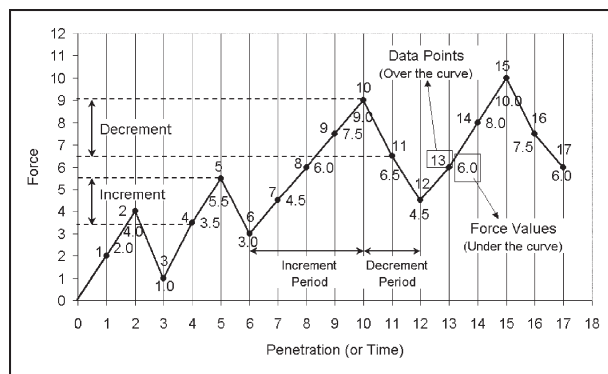
Therefore, the increment periods (or the number of incrementing points for a certain indentation penetration) of a brittle material might be shorter compared to a ductile material. If a material shows ductile characteristics, it would not break frequently, it would take mostly plastic and some elastic deformation, and its increment periods might be longer. The increment and decrement periods (or the number of incrementing and decrementing points) might vary depending on the size of the chips, cracks and crushed zone and the violence of the breakage. Larger chips and disturbance of the crushed (compacted) zone due to violence of the chipping might increase the decrement periods. Based on these considerations, it can be concluded that the percentage of the incrementing (or decrementing) data points on the total data points in an indentation test might be a measure of the breakage characteristic of the rocks.

Rate of force increment is also important when analysing the behaviour of a rock sample under indentation loading. Force increment rate per unit penetration (or unit time) might be an indicator of indentation forces and brittleness, or breakage characteristics. Force increment rate might also vary depending on the size of the chips, cracks and crushed zone and the violence of the breakage.

Quantification of force-penetration data in this study is based on the assumption that force-penetration signals obtained from indentation tests are random and stationary (time-independent). Random signals can be classified and manipulated in terms of their statistical properties. Terminology related to quantification of the increment and decrement rates and force increment and decrement periods is presented in Figure 3 in a simplified way and explained below[12-13].

If the force value ($F_i$) at the $i$th data point is higher than force value ($F_{i-1}$) at a previous data point ($i$-1th), the $i$th data point is an increment point. Force increment rate at the point $i$ is calculated as the force difference between these two data points ($F_i$-$F_{i-1}$), in force/unit time. Unit time can be the time difference between these data points, which is data sampling rate, or it can be converted to any other time unit. Average force increment rate ($F_{inc}$) is calculated for the entire graph, as follows:

$$F_{inc} = \frac{1}{k} \sum_{i=1}^{k} \left( F_i - F_{i-1} \right) \qquad [1]$$

# A set of indices based on indentation tests for assessment

where, $i$ is the subscript showing the numbers of individual increment points and $i = 1,2,....,k,$ and $k$ is the total number, of increment points over the entire graph.

If the force value ($F_j$) at the $j$th data point is lower than the force value ($F_{j-1}$) at a previous data point ($j$-1th), the $j$th data point is a decrement point. Force decrement rate at the point $j$ is calculated as the force difference between these two data points ($F_{j-1}-F_j$), in force/unit time. Average force decrement rate ($F_{dec}$) is calculated for the entire graph, as follows:

$$F_{dec} = \frac{1}{m} \sum_{j=1}^{m} \left( F_{j-1} - F_j \right) \quad [2]$$

where, $j$ is the subscript showing the numbers of individual decrement points and $j = 1,2,....,m,$ and $m$ is the total number of decrement points over the entire graph.

The number of sequential force increment points up to a decrement point is defined as a force increment period ($Pinc_p$). Since the data sampling rate is known, $Pinc_p$ is presented in unit time. The average force increment period ($P_{inc}$), see Figure 3, is calculated as follows:

$$P_{inc} = \frac{1}{n} \sum_{p=1}^{n} Pinc_p \quad [3]$$

where, $p$ is the subscript showing the numbers of individual increment periods, $p = 1,2,....,n,$ and $n$ is the total number of increment periods over the entire graph.

The number of sequential force decrement points up to an increment point is called a force decrement period ($Pdec_t$), in unit time. The average force decrement period ($P_{dec}$), see Figure 3, is calculated as follows:

$$P_{dec} = \frac{1}{s} \sum_{t=1}^{s} Pdec_t \quad [4]$$

where, $t$ is the subscript showing the numbers of individual decrement periods, $t = 1,2,....,s,$ and $s$ is the total number of decrement periods over the entire graph.

Some indices related to indentation force and rock brittleness can be empirically developed depending on these definitions, as follows:

$$FI = mF_{dec} / kF_{inc} \quad [5]$$

$$BI = P_{dec} / P_{inc} \quad [6]$$

$$BI_1 = k / (m + k) \quad [7]$$

where, $FI$ is force index, $BI$ is brittleness index estimated from increment and decrement periods, $BI_1$ is brittleness index estimated from the count of decrement and increment data points and the other parameters in the equations are as described above. Anticipated values of these unitless indices are between 0 and 1. Lower $FI$ and $BI$ values and higher $BI_1$ values are expected to represent relatively more brittle rocks. Since $BI$ and $BI_1$ are inherently similar indices, only the index $BI$ is presented in this study.

## Experimental set-up and procedures

Many mine visits were performed in Turkey within the scope of this study, and eleven large blocks of rock samples were collected from some of the operating mines in Turkey and subjected to a set of indentation tests, full-scale rock cutting tests and physical and mechanical property tests[13]. The physical and mechanical property tests were conducted to know the general characteristics of the rocks. Indentation tests were conducted for calculation of the force and brittleness indices. The linear cutting tests were conducted to validate the concept of force and brittleness indices mentioned above. The samples included harzburgite, serpentinite, trona, two different sandstone samples, siltstone, limestone, claystone, and three different chromite ore samples. All the linear cutting tests and physical and mechanical property tests were conducted in the laboratories of the Mining Engineering Department of the Istanbul Technical University. The linear cutting tests for limestone, sandstone-1, sandstone-2, and siltstone were conducted by K. Kel et al.[42] and for the rest of the rocks by the authors of this study[43-44] and previously published for different purposes.

### Physical and mechanical property tests

Uniaxial compressive strength, Brazilian tensile strength and dynamic elasticity modulus (acoustic velocity) tests were performed according to ISRM suggestions[45] using standard NX core samples. Schmidth hammer tests were performed as in the mines by using an N-type Schmidth hammer.

### Indentation tests

Indentation testing equipment used in this study consisted of a stiff MTS machine with a load capacity of 500 kN that presses an indentation tip to a pre-cast core sample. The indentation tests were conducted in the laboratories of the Mining Engineering Department of the Middle East Technical University in Ankara. The core diameter was standard NX diameter of around 53 mm. Core length to diameter ratio was
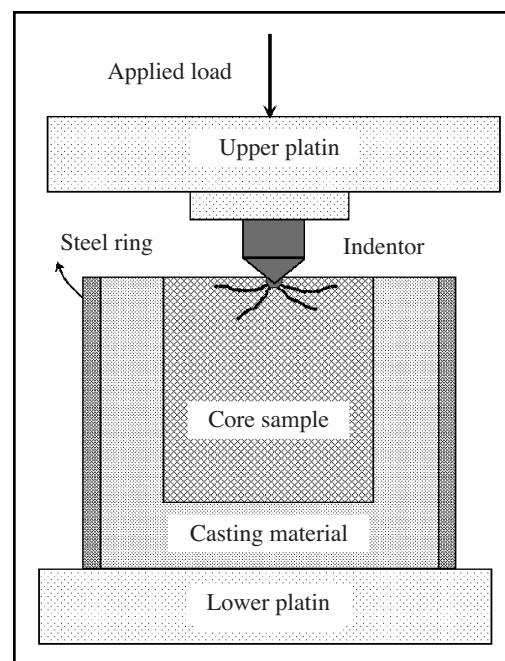
**Figure 4—Indentation testing set-up(simultaneous recording of indentation force and penetration at 1 Hz sampling rate)**

kept at least 1.5. The indentation tip was made of tungsten carbide and had conical shape with a tip angle of 75° and a blunting radius of 3 mm. Penetration was controlled at a constant rate of 0.0125 mm/s during the loading and when total penetration reached 9 mm, the testing was stopped. A generalized drawing of the indentation testing set-up is shown in Figure 4.

### Full-scale linear cutting tests

The linear cutting machine used in this study was recently built in the Mining Engineering Department of Istanbul Technical University based on a project supported by NATO[46], Figure 5. The independent linear cutting test variables consist of three major variables: rock type (11 rock blocks mentioned above), depth of cut, and cutter spacing. The dependent variables were mean and maximum cutter forces (cutting and normal forces), specific energy values, coarseness index, and size distribution of rock cuttings. The constant variables through the testing programme were cutting sequence (single-start), attack angle (56°), cutting speed (12.7 cm/s), skew angle (0°), tilt angle (0°), cutter type (Sandvik-35/80H), and data sampling rate (2000 Hz). The replication number for each test was at least three.

Unrelieved and relieved cutting modes are explained in Figures 6. There is no interaction between cutting grooves in the case of unrelieved cutting, which is opposed to the relieved cutting mode. By using the relieved cutting test results, the variation of specific energy with the ratio of cutter spacing to depth of cut is graphed as shown in Figure 6. This graph is used to find out the optimum cutting conditions (minimum specific energy) at which the machine excavates the rock in the most energy efficient manner.

Unrelieved cuts were performed prior to relieved cuts. Cutter (line) spacing to depth of cut ratios were maintained as 1, 2, 3 and 5 through the testing programme for the relieved cutting tests. Depth of cut *(d)* values were 5 and 9 mm for both relieved and unrelieved cuts. However, additional tests for unrelieved condition were included at 3 mm and 7 mm for limestone, claystone, sandstone-1, sandstone-2 and siltstone samples.
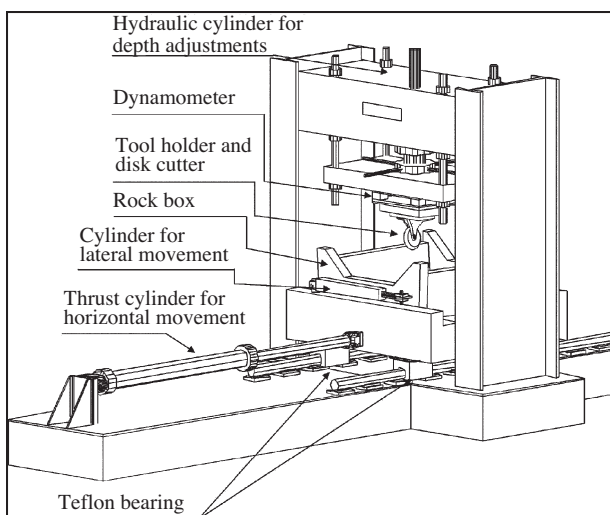


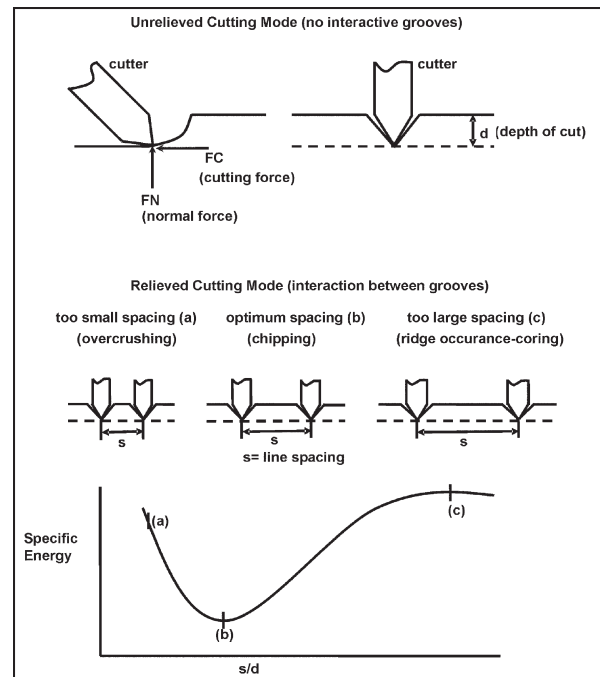Figure 5—Schematic drawing of the linear cutting testing set-up



**Figure 6—Unrelieved and relieved cutting modes and effect of ratio of line spacing to depth of cut (*s/d*) on specific energy**

All the tests were carried out with a conical cutter of S-35/80H manufactured by Sandvik. It had a gage of 80 mm, flange diameter of 64 mm, shank diameter of 35 mm, tip diameter of 22 mm and primary tip angle of 80°.

The samples of rock cuttings were collected from each cut and sieved by a set of sieves to get their size distribution and to estimate coarseness index. The sieves used were 25, 8, 2, 0.5, 0.125 mm and the pan. The sum of the cumulative retained percentages of material in the sieve size fractions give the coarseness index for each cut[4]. Table I summarizes an example estimation for the coarseness index for the medium-grade chromite sample at 9 mm depth of cut and optimum cutting condition. The higher coarseness index meant higher coarse material amounts and more efficient cutting. In this study, it was assumed that the higher coarseness index meant higher brittleness.

*Table I*

**Example estimations for coarseness index**

| Sieve Size | Retained | | |
| | Weight | Percentage | Cumulative |
| ( mm ) | ( g ) | ( % ) | ( % ) |
| +25 | 117.30 | 8.63 | 8.63 |
| -25 +8 | 679.75 | 50.02 | 58.66 |
| -8 +2 | 284.87 | 20.96 | 79.62 |
| -2 +0.5 | 111.43 | 8.20 | 87.82 |
| -0.5 +0.125 | 115.98 | 8.54 | 96.36 |
| -0.125 (pan) | 49.51 | 3.64 | 100.00 |
| Sum | 1359 | 100 | 431 |
| Coarseness Index | | | 431 |

Specific energy is a measure of the cutting efficiency and defined as the work done to cut a unit volume of rock. Since the cutting force removes (or excavates) the rock, specific energy[3] is a function of cutting force and yield and is calculated by Equation [8]:

$$SE = \frac{Fc}{Q} \qquad [8]$$

where, $SE$ is specific energy, $F_C$ is cutting force, Q is yield (excavated volume) per unit cutting length. The instantaneous cutting rate[2-3] of a mechanical miner using pick cutters is then estimated:

$$ICR = k\frac{P}{SE_{opt}} \qquad [9]$$

where, $ICR$ is instantaneous cutting rate, $P$ is cutting power of the mechanical miner, $SE_{opt}$ is specific energy at optimum cutting conditions, and $k$ is energy transfer coefficient depending on the mechanical miner utilized.

## Results and discussions

Some of the physical and mechanical properties of the rocks are summarized in Table II. As seen, the range varies from soft to hard and nonabrasive to abrasive rocks and minerals: uniaxial compressive strengths from 30 to 174 MPa, Brazilian tensile strengths from 2.2 to 11.6 MPa, and Cerchar abrasivity indices up to 4.1. Rock hardness (or strength) and abrasivity considerably affect the cutting performance. In rock cutting mechanics, the rocks that can be cut effectively by the pick cutters, such as conical or radial cutter are usually defined as soft rocks. Drag cutters can cut effectively, usually the soft (up to 100 to 120 MPa uniaxial compressive strength) and nonabrasive and/or moderately abrasive (up to 2 to 2.5 Cerchar abrasivity index) rocks. Harder and abrasive rocks can be usually cut effectively, in usual, by the roller cutters such as disc and button cutters.

The overall indentation test results and brittleness and force indices are summarized in Table III. Pictures of a harzburgite and a high-grade chromite sample after indentation test and a plot of force-penetration are presented in Figures 7 and 8, respectively.

### Table II

### Summary of physical and mechanical properties of rock samples

| Rock | $\gamma$ (g/cm$^3$) | UCS (MPa) | BTS (MPa) | $E_{sta}$ (GPa) | $V_p$ (km/s) | $E_{dyn}$ (GPa) | SHRV | CAI |
|---|---|---|---|---|---|---|---|---|
| Harzburgite | 2.65 | 58 | 5.5 | 2.1 | 3.14 | 16.1 | 47 | 0.8 |
| Serpentinite | 2.49 | 38 | 5.7 | 2.3 | 2.96 | 13.9 | 52 | 1.0 |
| Trona | 2.13 | 30 | 2.2 | 3.4 | 4.93 | 3.7 | 39 | - |
| Limestone | 2.72 | 121 | 7.8 | 57.0 | 3.91 | 37.9 | 55 | 1.4 |
| Claystone | - | 58 | 5.6 | - | - | - | - | - |
| Sandstone-1 | 2.65 | 114 | 6.6 | 17.0 | 3.74 | 36.5 | 53 | 4.1 |
| Sandstone-2 | 2.67 | 174 | 11.6 | 28.0 | 5.33 | 62.2 | 57 | 2.4 |
| Siltstone | 2.65 | 58 | 5.3 | 30 | 4.95 | 48.8 | 48 | 2.9 |
| High-Grade* Chromite | 4.03 | 32 | 3.7 | 3.5 | 3.48 | 31.2 | 30 | 2.1 |
| Medium-Grade* Chromite | 3.39 | 47 | 4.5 | - | 5.83 | 76.4 | 43 | 1.6 |
| Low-Grade* Chromite | 2.88 | 46 | 3.7 | 2.9 | 4.48 | 35.2 | 43 | 2.4 |

$\gamma$ = Density, $UCS$ = Unconfined Compressive Strength, $BTS$ = Brazilian Tensile Strength,
$E_{sta}$ = Static Elasticity Modulus, $V_p$ = Acoustic P-Wave Velocity $E_{dyn}$ = Dynamic Elasticity Modulus,
$SHVR$ = Schmidth Hammer Rebound Value ( N Type Hammer ), $CAI$ = Cerchar Abrasivity Index

(*) Since the grade of the chromite affects the structure and cuttability of the samples, the chromite samples are distinguished from each other as high-, medium- and low-grade samples. High-, medium- and low-grade samples used in this study include 46 to 50%, 42 to 46%, and 20 to 25% CR$_2$O$_3$, respectively.

### Table III

### Summary of indentation test results and index estimations

| Rock | Harzburgite | Serpentinite | Trona | Limestone | Claystone | Sandstone-1 | Sandstone-2 | Siltstone | HG* Chromite | MG* Chromite | LG* Chromite |
|---|---|---|---|---|---|---|---|---|---|---|---|
| Test Replication Number | 3 | 3 | 3 | 3 | 3 | 3 | 3 | 3 | 3 | 3 | 3 |
| $k$ = Increment Data Count | 1565 | 1400 | 1660 | 943 | 1589 | 951 | 1463 | 1501 | 1415 | 1482 | 1581 |
| $m$ = Decrement Data Count | 622 | 616 | 761 | 322 | 624 | 373 | 583 | 630 | 779 | 802 | 732 |
| $F_{inc}$ = Average Force Increment Rate ( kN/s ) | 0.072 | 0.061 | 0.098 | 0.089 | 0.084 | 0.069 | 0.077 | 0.058 | 0.062 | 0.063 | 0.063 |
| Standard Deviation ( kN/s ) | 0.056 | 0.046 | 0.101 | 0.060 | 0.062 | 0.052 | 0.058 | 0.045 | 0.050 | 0.053 | 0.047 |
| Maximum Force Increment Rate ( kN/s ) | 0.300 | 0.229 | 0.656 | 0.290 | 0.392 | 0.252 | 0.290 | 0.270 | 0.254 | 0.305 | 0.249 |
| $F_{dec}$ = Average Force Decrement Rate ( kN/s ) | 0.095 | 0.084 | 0.161 | 0.151 | 0.129 | 0.091 | 0.107 | 0.085 | 0.079 | 0.066 | 0.079 |
| Standard Deviation ( kN/s ) | 0.167 | 0.118 | 0.254 | 0.287 | 0.290 | 0.188 | 0.224 | 0.149 | 0.122 | 0.082 | 0.142 |
| Maximum Force Decrement Rate ( kN/s ) | 1.592 | 0.997 | 2.004 | 2.022 | 2.294 | 1.640 | 1.999 | 1.470 | 1.353 | 0.834 | 1.678 |
| $k.F_{inc}$ = Sum of Increment Forces ( kN ) | 37.5 | 28.8 | 54.2 | 41.3 | 44.5 | 32.9 | 37.1 | 28.6 | 29.2 | 31.4 | 33.0 |
| $m.F_{dec}$ = Sum of Decrement Forces ( kN ) | 19.8 | 17.3 | 39.8 | 22.8 | 26.7 | 17.0 | 19.9 | 17.1 | 20.2 | 17.8 | 19.4 |
| $P_{inc}$ = Average Increment Period ( s ) | 3.99 | 3.50 | 2.84 | 4.73 | 4.12 | 3.71 | 4.41 | 3.37 | 3.40 | 3.01 | 3.36 |
| Standard Deviation ( s ) | 4.69 | 3.26 | 2.79 | 6.56 | 5.27 | 5.44 | 5.33 | 2.94 | 5.10 | 4.10 | 4.33 |
| Maximum Increment Period ( s ) | 35 | 17 | 23 | 35 | 36 | 41 | 38 | 15 | 38 | 32 | 37 |
| $P_{dec}$ = Average Decrement Period ( s ) | 1.60 | 1.51 | 1.30 | 1.60 | 1.62 | 1.47 | 1.65 | 1.40 | 1.87 | 1.63 | 1.57 |
| Standard Deviation ( s ) | 1.10 | 1.09 | 0.81 | 1.41 | 1.14 | 0.90 | 1.28 | 0.97 | 2.27 | 1.74 | 1.26 |
| Maximum Decrement Period ( s ) | 7.67 | 7.33 | 7.00 | 9.00 | 7.67 | 6.00 | 8.33 | 6.67 | 18.33 | 18.67 | 10.00 |
| $FI$ ** = $m.F_{dec}$ / $k.F_{inc}$ | 0.528 | 0.601 | 0.734 | 0.552 | 0.600 | 0.517 | 0.536 | 0.598 | 0.692 | 0.567 | 0.588 |
| $BI = P_{dec}$ / $P_{inc}$ | 0.399 | 0.437 | 0.460 | 0.340 | 0.395 | 0.395 | 0.388 | 0.416 | 0.561 | 0.544 | 0.466 |
| $BI_1 = k$ / ( m + k ) | 0.716 | 0.697 | 0.685 | 0.748 | 0.718 | 0.719 | 0.721 | 0.706 | 0.645 | 0.649 | 0.684 |

( * ) HG = High-Grade, MG = Medium-Grade, LG = Low-Grade; ( ** ) The result is divided by the replication number.



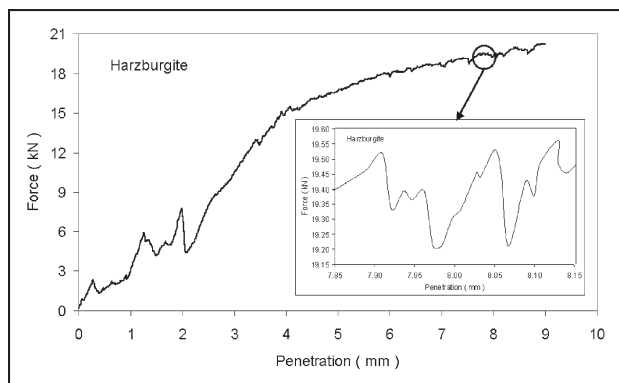Figure 7—A harzburgite (left) and a high-grade chromite (right) sample after indentation testing



Figure 8—Force-penetration graph of a harzburgite sample after indentation testing

Average increment periods vary between 2.84 seconds (trona) and 4.73 seconds (limestone), reaching maximum values up to 41 seconds (sandstone-1). Average decrement periods vary between 1.30 seconds (trona) and 1.87 seconds (high-grade chromite), reaching maximum values up to 18.67 seconds (medium-grade chromite). The standard deviation values are generally high (Table III), which might be due to the inherent characteristics of the rock breakage process. The indices $FI$ and $BI$ range from 0.517 (sandstone-1)

to 0.734 (trona), and from 0.340 (limestone) to 0.561 (high-grade chromite), respectively. Average force increment rates vary between 0.058 kN/s (siltstone) and 0.098 kN/s (trona), reaching maximum values up to 0.656 kN/s (trona). Average

force decrement rates vary between 0.066 kN/s (medium-grade chromite) and 0.161 kN/s (trona), reaching maximum values up to 2.294 kN/s (claystone).

The results of linear cutting tests are summarized for unrelieved cutting conditions in Table IV and related sieve analysis results in Table V. The results of linear cutting tests are summarized for optimum cutting conditions (relieved cutting at optimum *s/d* condition for each rock) in Table VI and related sieve analysis results in Table VII. An example of the relieved cutting results for medium-grade chromite is presented in Figure 9.

*Table IV*

**Summary of linear cutting test results for unrelieved cutting**

| Rock | Depth of Cut (mm) | Mean Forces Cutting (kgf) | Mean Forces Normal (kgf) | Peak Forces Cutting (kgf) | Peak Forces Normal (kgf) | Mean Specific Energy (kWh/m³) |
|---|---|---|---|---|---|---|
| Harzburgite | 5 | 531 | 621 | 1497 | 1447 | 18.6 |
| | 9 | 922 | 952 | 2691 | 2188 | 9.4 |
| Serpentinite | 5 | 295 | 326 | 785 | 883 | 9.5 |
| | 9 | 710 | 823 | 2015 | 1760 | 8.1 |
| Trona | 5 | 139 | 215 | 388 | 490 | 8.7 |
| | 9 | 420 | 639 | 1226 | 1380 | 6.7 |
| Limestone | 3 | 395 | 763 | 1184 | 1528 | 31.7 |
| | 5 | 746 | 1254 | 2151 | 2728 | 19.2 |
| | 9 | 1217 | 2041 | 3285 | 3892 | 16.4 |
| Claystone | 3 | 119 | 114 | 382 | 335 | 13.0 |
| | 5 | 301 | 297 | 897 | 820 | 14.1 |
| | 7 | 323 | 280 | 1099 | 892 | 7.9 |
| | 9 | 535 | 390 | 1692 | 1107 | 6.6 |
| Sandstone-1 | 3 | 391 | 441 | 913 | 878 | 47.2 |
| | 5 | 758 | 786 | 1969 | 1604 | 23.4 |
| | 9 | 992 | 869 | 2952 | 2189 | 13.5 |
| Sandstone-2 | 3 | 410 | 609 | 920 | 1192 | 54.3 |
| | 5 | 820 | 1084 | 2325 | 2386 | 49.6 |
| | 9 | 1686 | 1929 | 4810 | 4285 | 21.4 |
| Siltstone | 3 | 313 | 442 | 748 | 1041 | 42.1 |
| | 5 | 741 | 959 | 2304 | 2293 | 24.0 |
| | 9 | 843 | 863 | 3200 | 2410 | 15.5 |
| High-Grade Chromite | 5 | 279 | 231 | 716 | 552 | 11.1 |
| | 9 | 530 | 354 | 1483 | 923 | 5.8 |
| Medium-Grade Chromite | 5 | 347 | 302 | 1021 | 786 | 14.8 |
| | 9 | 931 | 666 | 2649 | 1649 | 12.0 |
| Low-Grade Chromite | 5 | 319 | 285 | 871 | 714 | 11.7 |
| | 9 | 663 | 572 | 1624 | 1185 | 11.0 |

*Table VI*

**Summary of linear cutting test results for relieved cutting at optimum ratio of line spacing to depth of cut**

| Rock | Mean Forces Cutting (kgf) | Mean Forces Normal (kgf) | Peak Forces Cutting (kgf) | Peak Forces Normal (kgf) | Mean Specific Energy (kWh/m³) | Optimum (s/d)* Ratio |
|---|---|---|---|---|---|---|
| Depth of Cut = 5 mm | | | | | | |
| Harzburgite | 478 | 518 | 1481 | 1362 | 12.9 | 5 |
| Serpentinite | 211 | 210 | 839 | 735 | 7.0 | 3 |
| Trona | 105 | 152 | 313 | 381 | 6.0 | 3 |
| Sandstone-1 | 656 | 692 | 1893 | 1609 | 15.9 | 5 |
| High-Grade Chromite | 242 | 213 | 838 | 704 | 9.3 | 3 |
| Medium-Grade Chromite | 255 | 224 | 669 | 549 | 12.8 | 2 |
| Low-Grade Chromite | 277 | 241 | 803 | 667 | 10.4 | 3 |
| Depth of Cut = 9 mm | | | | | | |
| Harzburgite | 911 | 944 | 2611 | 2273 | 8.4 | 5 |
| Serpentinite | 444 | 484 | 1406 | 1281 | 6.2 | 3 |
| Trona | 222 | 294 | 909 | 862 | 2.7 | 3 |
| Limestone | 1162 | 1728 | 3289 | 3640 | 12.0 | 5 |
| Claystone | 386 | 270 | 1243 | 858 | 6.0 | 2 |
| Sandstone-1 | 848 | 872 | 2517 | 1896 | 13.3 | 5 |
| Sandstone-2 | 942 | 1150 | 2835 | 2614 | 15.3 | 2 |
| Siltstone | 629 | 720 | 2176 | 2056 | 9.6 | 3 |
| High-Grade Chromite | 395 | 272 | 1425 | 887 | 3.9 | 3 |
| Medium-Grade Chromite | 641 | 448 | 1833 | 1194 | 6.4 | 2 |
| Low-Grade Chromite | 455 | 363 | 1404 | 1028 | 5.0 | 3 |

(*) *s* = Cutter Spacing, *d* = Depth of Cut

*Table V*

**Summary of sieve analysis results for unrelieved cutting**

| Sieve Size (mm) ➔ | +25 | -25 +8 | -8 +2 | -2 +0.5 | -0.5 +0.125 | -0.125 (pan) | Coarseness Index | Depth of Cut (mm) |
|---|---|---|---|---|---|---|---|---|
| Harzburgite | 0.0 | 46.1 | 34.8 | 9.7 | 5.9 | 3.5 | 414 | 5 |
| | 14.2 | 54.3 | 19.3 | 6.6 | 3.5 | 2.1 | 463 | 9 |
| Serpentinite | 0.0 | 20.9 | 51.0 | 18.5 | 6.5 | 3.1 | 380 | 5 |
| | 0.0 | 48.7 | 36.2 | 10.0 | 3.3 | 1.8 | 427 | 9 |
| Trona | 0.0 | 28.8 | 43.0 | 10.4 | 12.0 | 5.8 | 377 | 5 |
| | 0.0 | 61.0 | 20.4 | 7.5 | 10.3 | 0.8 | 430 | 9 |
| Limestone | 0.0 | 10.9 | 42.8 | 20.0 | 17.5 | 8.8 | 330 | 3 |
| | 0.0 | 38.3 | 39.6 | 12.1 | 6.9 | 3.1 | 403 | 5 |
| | 9.6 | 41.3 | 31.2 | 9.9 | 5.3 | 2.7 | 432 | 9 |
| Sandstone-1 | 0.0 | 1.3 | 40.6 | 21.5 | 24.2 | 12.4 | 294 | 3 |
| | 0.0 | 51.9 | 22.2 | 9.9 | 10.8 | 5.2 | 405 | 5 |
| | 40.4 | 32.4 | 11.7 | 6.0 | 6.2 | 3.3 | 485 | 9 |
| Sandstone-2 | 0.0 | 0.7 | 48.1 | 20.7 | 18.8 | 11.7 | 307 | 3 |
| | 0.0 | 25.1 | 40.5 | 12.9 | 13.0 | 8.5 | 361 | 5 |
| | 7.7 | 47.2 | 22.4 | 9.2 | 8.3 | 5.2 | 421 | 9 |
| Siltstone | 0.0 | 3.9 | 58.8 | 16.5 | 10.7 | 10.1 | 336 | 3 |
| | 3.3 | 49.9 | 29.7 | 7.9 | 4.7 | 4.5 | 426 | 5 |
| | 10.9 | 52.2 | 21.7 | 7.0 | 4.1 | 4.1 | 446 | 9 |
| High-Grade Chromite | 0.0 | 5.5 | 21.1 | 35.7 | 28.3 | 9.4 | 285 | 5 |
| | 5.3 | 27.5 | 19.5 | 23.8 | 18.6 | 5.3 | 361 | 9 |
| Medium-Grade Chromite | 0.0 | 11.5 | 31.1 | 26.8 | 20.8 | 9.8 | 314 | 5 |
| | 6.1 | 29.5 | 23.5 | 19.2 | 15.8 | 5.9 | 373 | 9 |
| Low-Grade Chromite | 0.0 | 40.9 | 35.4 | 10.4 | 7.9 | 5.4 | 398 | 5 |
| | 3.4 | 56.2 | 20.7 | 8.0 | 7.4 | 4.3 | 427 | 9 |

*Table VII*

**Summary of sieve analysis results for relieved cutting at optimum ratio of line spacing to depth of cut**

| Sieve Size (mm) ➔ | +25 | -25 +8 | -8 +2 | -2 +0.5 | -0.5 +0.125 | -0.125 (pan) | Coarseness Index |
|---|---|---|---|---|---|---|---|
| Depth of Cut = 5 mm | | | | | | | |
| Harzburgite | 0.0 | 54.8 | 26.7 | 9.3 | 5.6 | 3.7 | 423 |
| Serpentinite | 0.0 | 34.0 | 46.4 | 13.0 | 4.4 | 2.2 | 406 |
| Trona | 0.0 | 38.5 | 38.1 | 10.0 | 8.6 | 4.8 | 397 |
| Sandstone-1 | 7.6 | 51.2 | 18.3 | 9.0 | 9.3 | 4.6 | 425 |
| High-Grade Chromite | 0.0 | 16.9 | 26.6 | 25.8 | 21.0 | 9.7 | 320 |
| Medium-Grade Chromite | 0.0 | 12.4 | 38.0 | 22.6 | 18.1 | 8.9 | 327 |
| Low-Grade Chromite | 0.0 | 50.0 | 29.0 | 9.7 | 8.0 | 3.4 | 414 |
| Depth of Cut = 9 mm | | | | | | | |
| Harzburgite | 11.0 | 62.5 | 16.4 | 7.0 | 1.3 | 1.8 | 468 |
| Serpentinite | 0.0 | 55.5 | 30.3 | 8.9 | 3.5 | 1.8 | 434 |
| Trona | 28.4 | 48.1 | 13.0 | 4.6 | 4.3 | 1.6 | 487 |
| Limestone | 32.1 | 33.0 | 22.9 | 6.6 | 3.3 | 2.1 | 478 |
| Sandstone-1 | 24.1 | 46.6 | 13.8 | 5.8 | 6.1 | 3.6 | 466 |
| Sandstone-2 | 4.3 | 56.1 | 22.3 | 7.1 | 6.3 | 3.9 | 433 |
| Siltstone | 29.8 | 44.7 | 15.3 | 4.7 | 2.8 | 2.7 | 486 |
| High-Grade Chromite | 16.3 | 27.7 | 16.7 | 18.9 | 14.8 | 5.6 | 395 |
| Medium-Grade Chromite | 8.6 | 50.1 | 20.9 | 8.2 | 8.5 | 3.6 | 431 |
| Low-Grade Chromite | 21.7 | 48.3 | 15.3 | 6.2 | 5.5 | 3.1 | 465 |
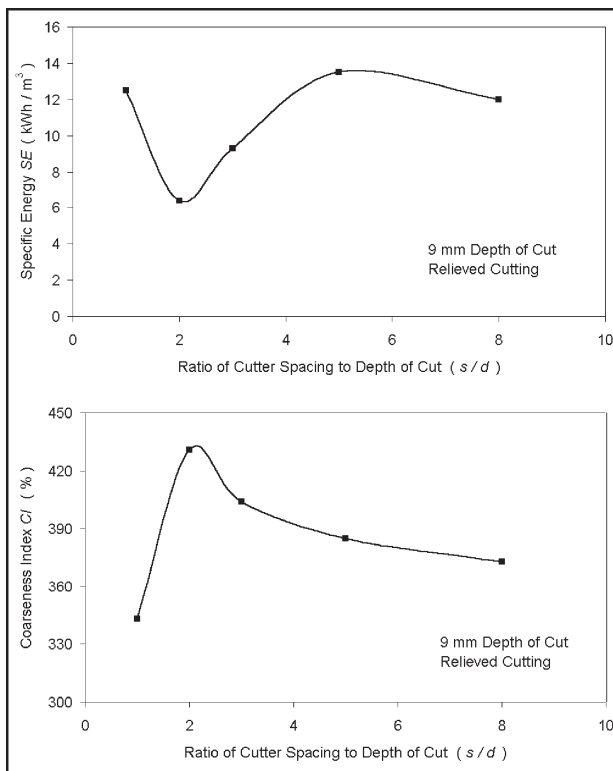
Figure 9—Relieved cutting test results for medium-grade chromite (s/d=8 presents unrelieved cutting)



Figure 10—Relationships between force index *FI* and cutting performance for 9 mm depth of cut and optimum cutting conditions

Curve fitting studies (with 95 per cent confidence level) indicate that the force index *FI* exhibits moderate relationships with the cutting and normal cutter forces, as well as specific energy values for optimum cutting conditions at 5 and 9 mm depth of cut values. An example of curve fitting studies is presented in Figure 10 for 9 mm depth of cut values and optimum cutting conditions. The data indicate some scatter, but it is possible to deduce a general trend. The same relationships are slightly less pronounced for the unrelieved cutting conditions, which might be due to high standard deviation values. The force index *FI* has quite weak or insignificant relationships with the coarseness index CI and sieve analysis results. This is anticipated since force index *FI* includes inherently force parameters (Equation [5]).

The relationship between the brittleness index *BI* and the coarseness index *CI* exhibits a general trend, (Figure 11) for unrelieved cutting conditions. Increase in the brittleness (lower *BI* values) increases the coarseness index. Although *BI* and *CI* have moderate correlation coefficients, the high-grade and medium-grade chromite data points can be considered to increase the correlation coefficients. Similar trends are observed for the relationships between *BI* and the coarse (assuming cumulative material greater than 2 mm and/or 8 mm) and fine material (assuming cumulative material less than 0.125mm and/or 0.5 mm) percentages. For the optimum cutting conditions, the relationship between *BI* and *CI* is less pronounced (although it is possible to deduce a general trend).

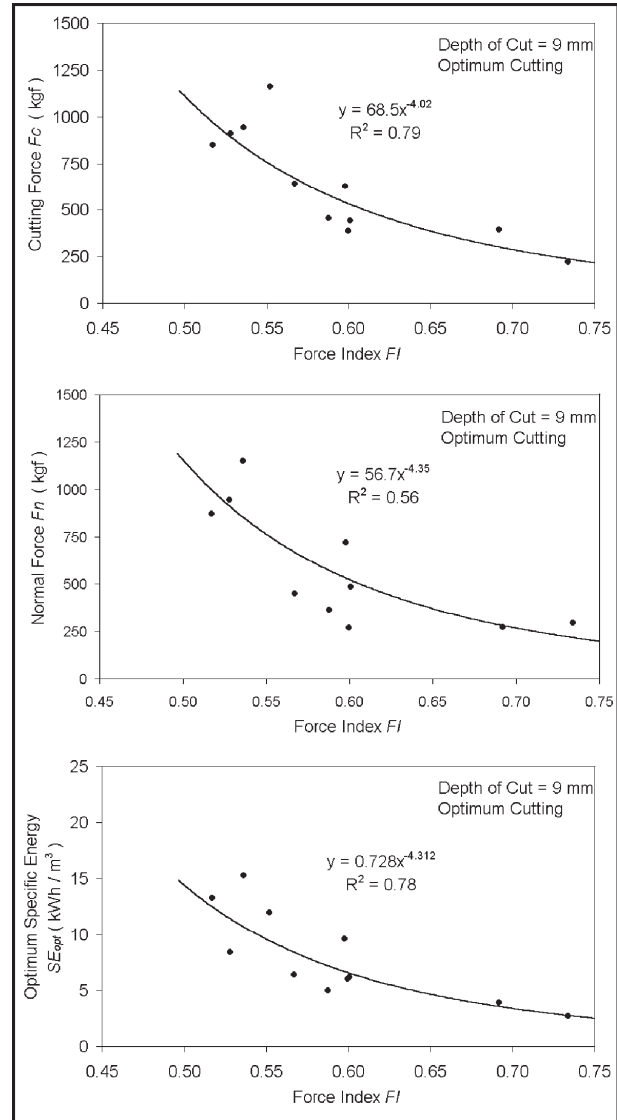The brittleness index *BI* has usually poorer relationships with the cutter forces and specific energy for all cutting conditions, although a general trend is present (an example in Figure 12 for 9 mm depth of cut and optimum cutting conditions).

In addition, *BI* and *BI*$_1$ are highly correlated with each other (with R2 value of 99 per cent). It is expected since they include similar parameters Equations [6] and [7]. The correlation between *BI* and *FI* is very low (with R2 value of 35 per cent), which is expected since they include different parameters Equations [5] and [6].

The most widely used brittleness indices[33-34] are presented in Equation [10]:

$$B_5 = \frac{\sigma_c}{\sigma_t} \quad \text{or} \quad B_6 = \frac{\sigma_c - \sigma_t}{\sigma_c + \sigma_t} \qquad [10]$$

where $B_5$ and $B_6$ are brittleness indices, and $\sigma_c$ and $\sigma_t$ are uniaxial compressive strength and Brazilian tensile strength of rock, respectively. No meaningful relationship can be found between $B_5$ (or $B_6$) and *BI, CI,* cutting force, normal force, and specific energy.
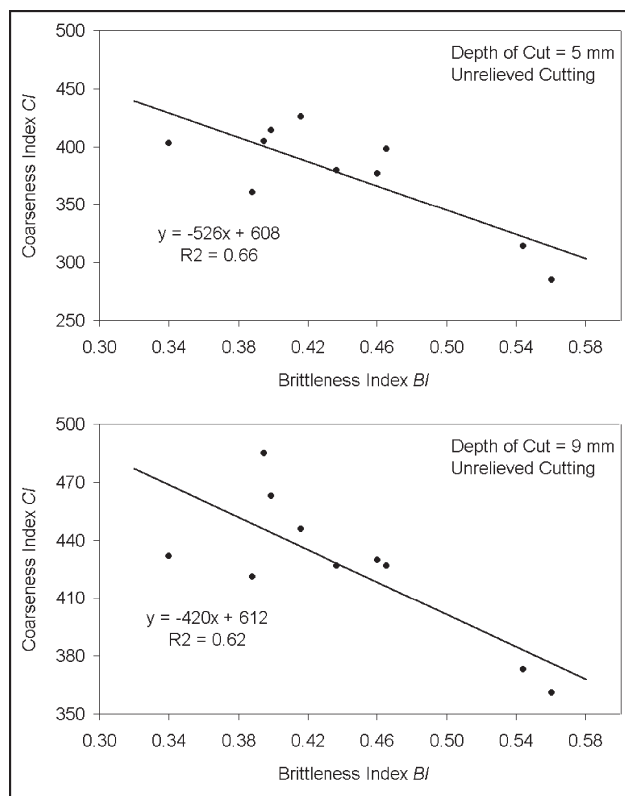
**Figure 11—Relationship between brittleness index *BI* and coarseness index *CI* for unrelieved cutting**



**Figure 12—Relationship between brittleness index *BI* and cutting performance for 9 mm depth of cut and optimum cutting conditions**

The relationships between mechanical properties of the rocks and the force index *FI* and the brittleness index *BI* are presented in Figures 13 and 14, respectively. The force index *FI* has moderate relationships with uniaxial compressive strength, Brazilian Tensile Strength and Schmidth Hammer Rebound Values (with $R^2$ values of 60, 63 and 58 per cent, respectively). The relationships for the brittleness index *BI* are also moderate (with $R^2$ values of 53 per cent for uniaxial compressive strength, 42 per cent for Brazilian Tensile Strength and 69 per cent for Schmidth Hammer Rebound Values).

## Conclusions

A set of new empirical indices were developed, which are useful for predicting cutting efficiency and mechanical properties of rocks, as well as rock brittleness relevant to rock cutting mechanics. A new interpretation method of macro-scale indentation tests is developed in this context. The basic advantage of this simple method is that it is based on core samples.

Results of the experimental works indicate that the force index *FI* is moderately correlated with cutting performance, i.e. cutting force, normal force and specific energy, in relieved and unrelieved cutting conditions. Force index *FI* is also moderately correlated to the mechanical properties of the rocks, i.e. uniaxial compressive strength, Brazilian Tensile Strength and Schmidth Hammer Rebound Value. However, it is correlated rather poorly with the coarseness index *CI* and coarse and fine material percentages for almost all cutting
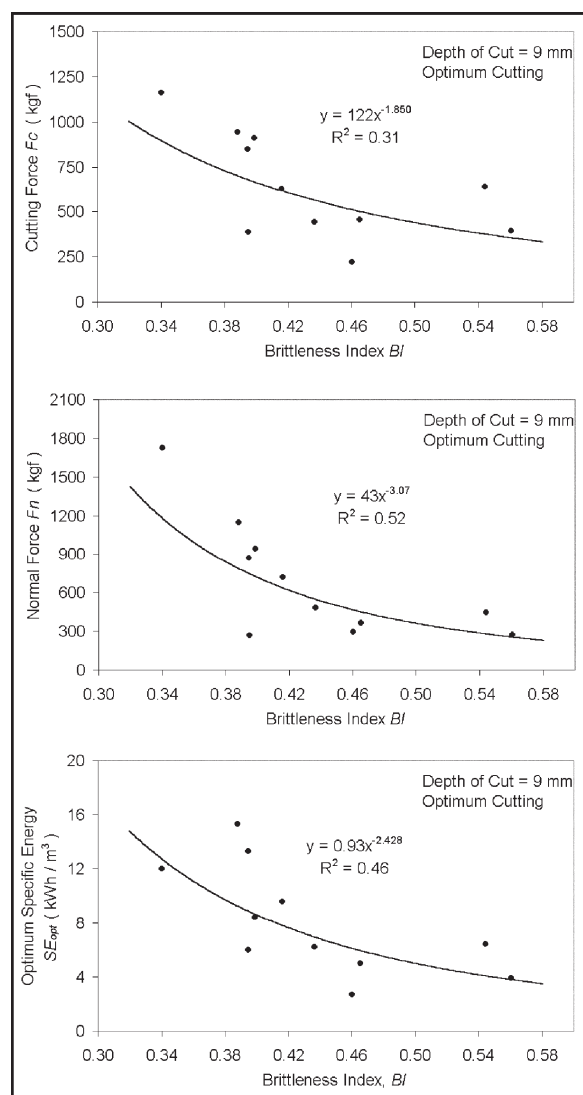
conditions. Therefore, the force index *FI* could be used as a parameter for prediction of cutting performance and mechanical properties of rocks.

The brittleness index *BI* exhibits moderate relationships with the cutting efficiency for unrelieved cutting conditions and mechanical properties of the rocks. The relationships are lower for relieved cutting conditions. Although the brittleness index *BI* is moderately correlated with the coarseness index *CI*, cutting performance and mechanical properties of the rocks, there is a gap between the data groups. Additional data are required to reliably use the brittleness index, as proposed in this study, as a predictive parameter.
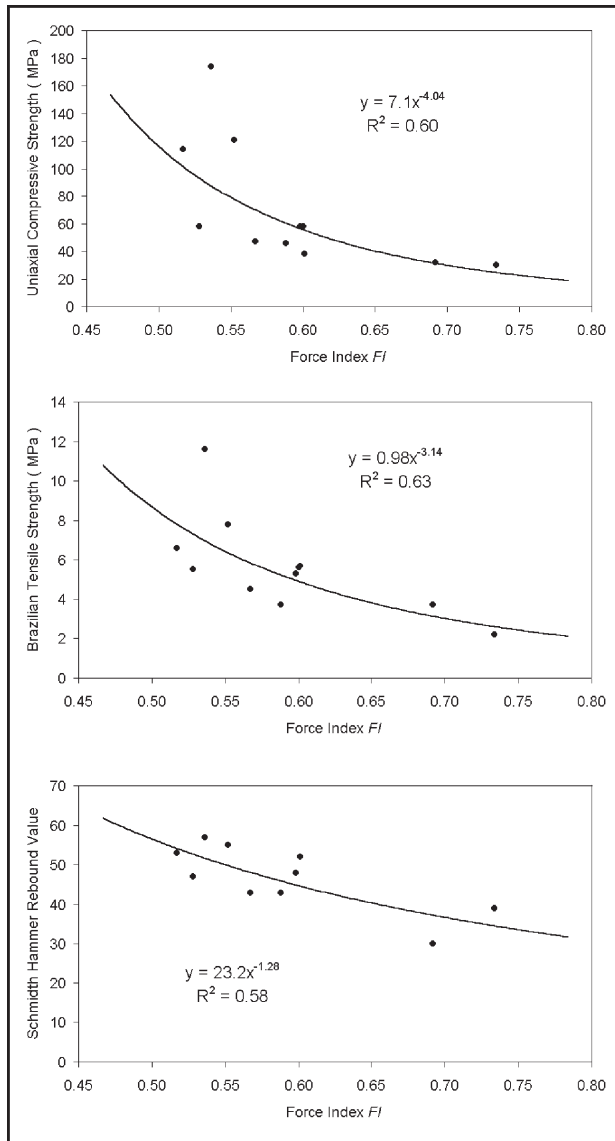
## Acknowledgements

**Figure 13—Relationship between force index *FI* and mechanical properties of the rocks**
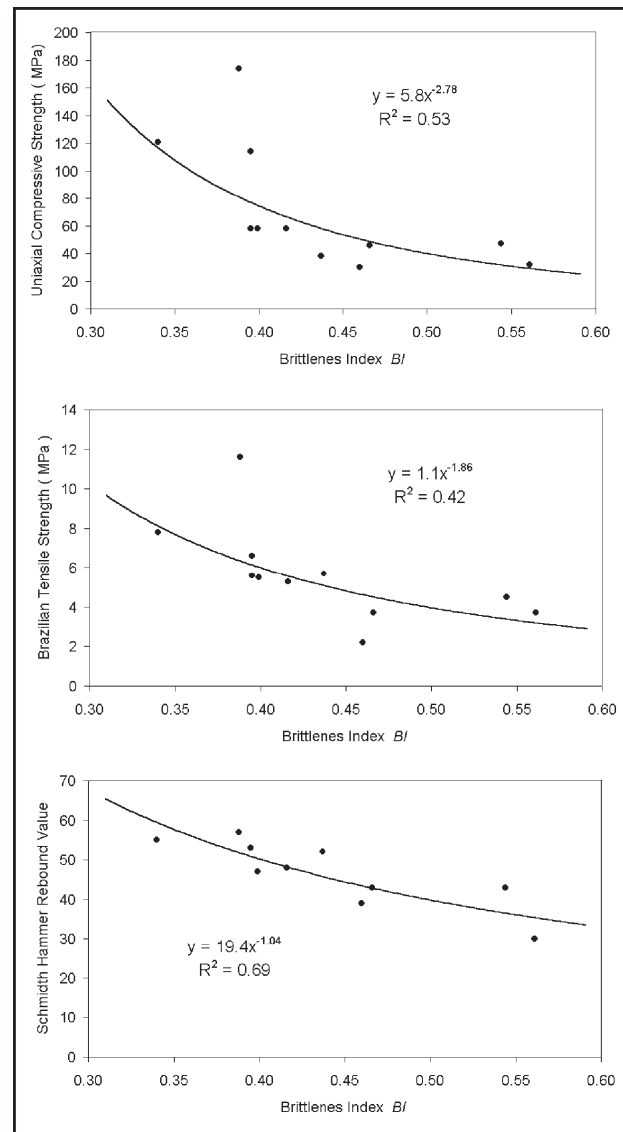


**Figure 14—Relationships between brittleness index *BI* and mechanical properties of the rocks**

## References

1. FOWELL, R.J. and SMITH, I.M. Factors influencing the cutting performance of a selective tunnelling machine. *Int. Tunnelling '76 Symp.*, 1-5 Mar., London, 1976. pp. 301–318.

2. MCFEAT-SMITH I. and FOWELL R.J. Correlation of rock properties and the cutting performance of tunnelling machines. *Conference on Rock Engineering,* UK, organized jointly by the British Geotechnical Society and Department of Mining Engineering, The University of Newcastle Upon Tyne, 1977. pp. 581–602.

3. ROXBOROUGH, F.F. Cutting rocks with picks. *The Mining Engineer,* June, 1973. pp. 445–454.

4. BILGIN, N. *Applied Rock Cutting Mechanics for Civil and Mining Engineers.* Birsen Publishing Co., Turkey 192 pp.

5. OZDEMIR, L. *Mechanical Mining. Short Course Notebook.* Colorado School of Mines, Mining Eng. Dept., 1995.

6. SINGH, S.P. Brittleness and the mechanical winning of coal. *Min. Sci. Tech.*, 3, 1986. pp. 173–180.

7. GOKTAN, M. Brittleness and micro-scale rock cutting efficiency. *Min. Sci. Tech.,* 13, 1991. pp. 237–241.

8. DEKETH, H.J.R., *et al.* Towards the prediction of rock excavation machine performance. *Bull. Eng. Geol. Env.,* No. 57, 1998. pp. 3–15.

9. VERHOEF, P.N.W., OCKELOEN, J.J. and KESTEREN, W.G.M.V. The significance of rock ductility for mechanical rock cutting. *2nd North American Rock Mechanics Symp.,* Montreal, Quebec, Canada, 19-21 June, 1996. pp. 709-716.

10. KAHRAMAN, S. Correlation of TBM and drilling machine performances with rock brittleness. *Engineering Geology,* 65, 2002. pp. 269–283.

11. UNIVERSITY OF TRONDHEIM, THE NORWEGIAN INSTITUTE OF TECHNOLOGY. Hard Rock Tunnel Boring. No: 1-94, 1994. 164 pp.

12. COPUR, H., TUNCDEMIR, H., BALCI, C. and OZTURK, A. A Brittleness Concept Based on Indentation Tests for Assessment of Rock Cuttability. *10th Int. Symp. on Mine Planning and Equipment Selection,* New Delhi-India, Nov. 19-21, R. K. Singhal, B.P. Singh (eds.), 2001. pp. 783–788.

13. COPUR, H., TUNCDEMIR, H., BALCI, C. and OZTURK, A. Investigation of the Parameters Affecting Rock Brittleness from the Rock Cutting Mechanics Point of View. TUBITAK Project No: INTAG-721, 2003.

14. EVANS, I. A theory of the basic mechanics of coal ploughing. *Int. Symp. on Mining Research,* vol.2, 1962. pp.761–798.

15. NISHIMATSU, Y. The mechanics of rock cutting. *Int. J. Rock Mech. Min. Sci.*, vol. 9, 1972. pp. 261–270.

16. EVANS, I. Basic mechanics of the point-attack pick. *Colliery Guardian,* May, 1984. pp. 189–193.

17. ROSTAMI, J. and OZDEMIR, L. A new model for performance prediction of hard rock TBMs. *Rapid Excavation and Tunnelling Conference,* 1993. pp. 793–809.

18. ROXBOROUGH, F.F. and PHILLIPS, H.R. Rock excavation by disc cutter. *Int. J. Rock. Mech. Min. Sci. & Geomechs. Abstr.*, vol. 12, 1975. pp. 361–366.

19. REICHMUTH, D. R. Correlation of force-displacement data with physical properties of rock for percussive drilling systems. *5th US Rock Mechanics Symp.,* Univ. Minnesota, C. Fairhurst (ed.), 1963. pp. 33–59.

20. CHETHAM, J.B. An analytical study of rock penetration by a single bit tooth. *8th Annual Drilling and Blasting Symp.*, Univ. Minnesota, 1958. pp. 1A–25A.

21. PAUL, B. and SIKARSKIE, D.L. A preliminary theory of static penetration by a rigid wedge into a brittle material. *Society for Mining, Metallurgy and Exploration, Transactions,* U.S.A.., Dec., 1965. pp. 372–383.

22. MILLER, M. H. and SIKARSKI, D.L. On the penetration of rock by three-dimensional indentors. *Int. J. Rock Mech. Min. Sci., vol. 5,* 1968. pp. 375–398.

23. LUNDBERG, B. Penetration of rock by conical indentors. *Int. J. Rock Mech. Min. Sci.,* 11, 1974. pp. 209–214.

24. LINDQVIST, P.A. and LAI, H.H. Behaviour of crushed zone in rock indentation. *Rock Mechanics and Rock Engineering,* vol. 16, 1983. pp. 199–207.

25. RANMAN, K.E. A model describing rock cutting with conical picks. *Rock Mechanics and Rock Engineering,* vol. 18, 1985. pp. 131–140.

26. PANG, S.S., GOLDSMITH, W. and HOOD, M. A force-indentation model for brittle rocks. *Rock Mechanics and Rock Engineering,* vol. 22, 1989. 127–148.

27. MISHNAEVSKY, L.L. Physical mechanisms of hard rock fragmentation under mechanical loading: a review. *Int. J. Rock Mech. Min. Sci. & Geomech. Abstr.,* vol. 32, 1995. pp. 763–766.

28. HUANG,, H., DAMJANAC, B. and DETOURNAY, E. Normal wedge indentation in rocks with lateral confinement. *Rock Mechanics and Rock Engineering*, vol. 31 no. 2, 1998. pp. 81–94.

29. MAURER, W.C. The state of rock mechanics knowledge in drilling. *8th Symp. on Rock Mechanics,* C. Fairhurst (ed.) AIME, New York, 1967. pp. 355–395.

30. DOLLINGER, G.L. Choosing cutters for the best boreability. *Compressed Air Magazine,* Sept., 1977. pp. 15–19.

31. DOLLINGER, G.L., HANDEWITH, H.J. and BREEDS, C.D. Use of the indentation tests for estimating TBM performance. *Canadian Tunneling,* The Annual Publication of The Tunneling Association of Canada, Lo, K. Y. (ed.), 1998. pp. 27–33.

32. KAHRAMAN, S., BALCI, C., YAZICI, S. and BILGIN, B. Prediction of the penetration rate of rotary blast hole drills using a new drillability index. *Int. J. Rock Mech. Min. Sci.,* vol. 37, 2000. pp. 729–743.

33. HUCKA, V. and DAS, B. Brittleness determination of rocks by different methods. *Int. J. Rock Mech. Min. Sci.,* vol. 11, 1974. pp. 389–392.

34. ANDREEV, G.E. *Brittle Failure of Rock Materials, Test Results and Constitutive Models.* A.A. Balkema, Rotterdam / Brookfield, 1995. 446 pp.

35. ALTINDAG, R. The evaluation of rock brittleness concept on rotary blast hole drills. *The J. of the South African Inst. of Min. and Metall.*, Jan-Feb., 2002. pp. 61–66.

36. ALTINDAG, R. Correlation of specific energy with rock brittleness concepts on rock cutting. *The J. of the South African Inst. of Min. and Metall.*, Apr., 2003. p. 163.

37. ALTINDAG, R. The useability of coarseness index in the prediction of penetration rate of percussive blasthole drills in a limestone opencast quarry. *1st Int. Symp. of the Istanbul Technical University Faculty of Mines on Earth Sciences and Engineering,* 16-18 May, Istanbul, Turkey, 2002. p. 196 (Abstract).

38. LAWN, B.R. *Fracture of Brittle Solids.* 2nd Ed., Cambridge University Press, 1993. p. 94, 378 pp.

39. QUINN, J.B. and QUINN, G.D. Indentation brittleness of ceramics: a fresh approach. *J. of Materials Sci.,* 1997. vol. 32, pp. 4331–4346

40. SEGHAL, J. and ITO, S. Brittleness of glass. *J. of Non-Crystalline Solids,* no. 253, 1999. pp. 126–132.

41. BOCCACCINI, A.R. Machinability and brittleness of glass-ceramics. *J. of Materials Processing Technology,* 1997. vol. 65, pp. 302–304.

42. KEL, K., AKCIN, N., TUNCDEMIR, H. and BILGIN, B. Cuttability characteristics of high strength rocks for roadheader selection in Zonguldak Coalfield. *10th Int. Symp. on Mine Planning and Equipment Selection,* New Delhi, India, Nov.19-21, R. K. Singhal, B.P. Singh (eds.), 2001. pp. 789–795.

43. BILGIN, N., COPUR, H., TUNCDEMIR, H., and BALCI, C. Investigations into the Applications of Roadheaders for the Production in Turkish Underground Metal Mines. DPT Project No: 141, 2002.

44. COPUR, H., TUNCDEMIR, H., BILGIN, N. and DINCER, T. Specific energy as a criterion for the use of rapid excavation systems in Turkish mines. *The Institution of Mining and Metallurgy,* Transactions Section-A Mining Technology, Nov-Dec, 2001. vol. 110, pp. A149–157.

45. BROWN, E.T. *ISRM Suggested Methods. Rock Characterization Testing and Monitoring.* Oxford, Pergamon Press, 1981.

46. ESKIKAYA, S., BILGIN N., OZDEMIR, L., NASUF, E., ÖKTEN, G., YAZICI, S., KUZU, C., ERGIN, H., AKGUL, M., DINCER, T., BALCI, C., TUNCDEMIR, H., ACAROGLU, O., AVSAR, S., OZBAKIR, O. and TUNCEL, Z. Development of Rapid Excavation Technologies for the Turkish Mining and Tunneling Industries. *NATO TU-Excavation SfS Programme Project Report.* Istanbul Technical University, Mining Eng. Dept., Preparation of Report by N. Bilgin and C. Balci, Sept., 2000. 172 pp. ◆